4,8,12,16-Tetra-*tert*-butyl-*s*-indaceno[1,2,3-*cd*:5,6,7-*c′d′*]diphenalene: A Four-Stage Amphoteric Redox System

Kenji Ohashi, Takashi Kubo, Takashi Masui, Kagetoshi Yamamoto,* Kazuhiro Nakasuji,* Takeji Takui,† Yasushi Kai,‡ and Ichiro Murata§

Contribution from Department of Chemistry, Graduate School of Science, Osaka University, Toyonaka, Osaka 560, Japan, Department of Applied Chemistry, Faculty of Engineering, Osaka University, Suita, Osaka 565, Japan, and Department of Chemistry, Faculty of Science, Osaka City University, Sumiyoshi-ku, Osaka 558, Japan

Received March 26, 1997

Abstract: A four-stage amphoteric redox hydrocarbon (**5**) containing two phenalenyl units was prepared. X-ray crystallography of **5** reveals a delocalized D_{2h} structure, which is consistent with the presence of only five signals in the ^{1}H NMR spectrum of **5** at −60 °C. The cyclic voltammogram of **5** exhibits four reversible redox waves with a small numerical sum (E_1^{sum}) of first oxidation (E_1^{ox}) and reduction (E_1^{red}) potentials. Four redox states of **5** were successfully generated from the neutral **5** and were characterized by NMR, ESR, and UV−vis−near-IR spectroscopies and theoretical calculations. These spectral data reveal that phenalenyl units play an important role in the high amphotericity of **5** and the stability of the redox states generated.

Introduction

Some conjugated hydrocarbons exhibit the amphoteric redox properties so that the molecule is oxidized and reduced by a multistage electron transfer.[1] To evaluate the amphoteric redox abilities of such a molecule, the numerical sum (E^{sum}) of the oxidation potential (E^{ox}) and the reduction potential (E^{red}), $E^{sum} = E^{ox} + (-E^{red})$, is used. In general, redox compounds with small E^{sum} values are easily oxidized and reduced and give thermodynamically stable redox species. In particular, a compound with nonbonding molecular orbitals (NBMO) will exhibit the highest redox ability because the addition or removal of electrons in the NBMO should not change the magnitude of the π-electron energy in a simple Hückel molecular orbital (HMO) approximation. A representative compound would be the phenalenyl radical **1**•, which possesses a thermodynamically stable cation (**1**$^+$) and anion (**1**$^-$) and exhibits the relatively small E_1^{sum} value of 1.6 V.[2] However, the open-shell phenalenyl radical suffers from a serious disadvantage, i.e., lack of kinetic stability. The phenalenyl radical, like ordinary radicals, tends to dimerize or to give oxidized species in the presence of air. Therefore, molecules with a closed-shell structure which retain the high redox ability of the phenalenyl species should develop stable redox compounds with a small E^{sum} value.

On the basis of these ideas, we designed and synthesized four-stage amphoteric redox hydrocarbons containing two phenalenyl units.[1c−f] All of these compounds exhibited high amphotericity and small E_1^{sum} values. In particular, pentaleno[1,2,3-*cd*:4,5,6-*c′d′*]diphenalene (PDPL, **2**),[1e] and 6,14-diisopropyl-*s*-indaceno-[1,2,3-*cd*:5,6,7-*c′d′*]diphenalene (DI-IDPL, **3**),[1f] gave extremely small E_1^{sum} values of 0.99 and 1.10 V, respectively. Although these compounds were designed to be the unstable structures in the neutral state, this instability should disappear in the oxidized and reduced species (Figure 1). Compound **2** contains the pentalene structure, while the *s*-indacene structure is included in the center of compond **3**. Both pentalenes and *s*-indacenes with 4nπ electrons on the periphery are known to be highly reactive compounds. Indeed, compound **2** shows the smallest E_1^{sum} value among the closed-shell hydrocarbons reported thus far.

Determining the magnitude of these E_1^{sum} value is the primary way to evaluate these amphoteric redox compounds, although another prominent feature of these componds is that they are expected to give *stable* reduced and oxidized species. Examples of these compounds which give one or two redox species abound; for example, neutral naphthalene is known to afford a radical anion and a radical cation.[5] Limited numbers of these

† Department of Applied chemistry, Faculty of Engineering, Osaka University.

‡ Osaka City University.

§ Current address: Fukui Institute of Technology, Gakuen, Fukui 910, Japan.

(1) (a) Hagenbruch, B.; Hesse, K.; Hünig, S.; Klug, G. *Justus Liebigs Ann. Chem.* **1981**, 256. (b) Hünig, S.; Hornaer, M.; Schilling, P. *Angew. Chem., Int. Ed. Engl.* **1975**, *14*, 556. (c) Nakasuji, K.; Yoshida, K.; Murata, I. *J. Am. Chem. Soc.* **1982**, *104*, 1432. (d) Nakasuji, K.; Yoshida, K.; Murata, I. *Chem. Lett.* **1982**, 969. (e) Nakasuji, K.; Yoshida, K.; Murata, I. *J. Am. Chem. Soc.* **1983**, *105*, 5136. (f) Murata, I.; Sasaki, S.; Klabunde, K.-U.; Toyoda, J.; Nakasuji, K. *Angew. Chem., Int. Ed. Engl.* **1991**, *30*, 172. See also: Parker, V. D. *J. Am. Chem. Soc.* **1976**, *98*, 98. Deuchert, K.; Hünig, S. *Angew. Chem., Int. Ed. Engl.* **1978**, *17*, 875. Takahashi, K.; Suzuki, T. *J. Am. Chem. Soc.* **1989**, *111*, 5483. Takahashi, K. *Pure. Appl. Chem.* **1993**, *65*, 127. Bachmann, R.; Gerson, F.; Gescheidt, G.; Vogel, E. *J. Am. Chem. Soc.* **1992**, *114*, 10855. Bachmann, R.; Gerson, F.; Gescheidt, G.; Vogel, E. *J. Am. Chem. Soc.* **1993**, *115*, 10286. Vogel, E.; Dörr, J.; Herrmann, A.; Lex, J.; Schmickler, H.; Walgenbach, P.; Gisselbrecht, J. P.; Gross, M. *Angew. Chem., Int. Ed. Engl.* **1993**, *32*, 1597.

(2) Nakasuji, K.; Yamaguchi, M.; Murata, I.; Yamaguchi, K.; Fueno, T.; Ohya-Nishiguchi, H.; Sugano, T.; Kinoshita, M. *J. Am. Chem. Soc.* **1989**, *111*, 9265.

(3) (a) Reid, D. H. *Quart. Rev.* **1965**, *19*, 274. (b) Gerson, F. *Helv. Chim. Acta* **1966**, *49*, 1463. (c) Prinzbach, H.; Freudenberger, V.; Scheidegger, U. *Helv. Chim. Acta* **1967**, *50*, 1087. (d) Sethson, I.; Johnels, D.; Edlund, U.; Sygula, A. *J. Chem. Soc., Perkin Trans 2.* **1990**, 1339.

(4) Hafner, K. *Angew. Chem., Int. Ed. Engl.* **1964**, *3*, 165. Dönges, R.; Hafner, K.; Lindner, H. J. *Tetrahedron Lett.* **1976**, 1345. Hafner, K.; Stowasser, B.; Krimmer, H.-P.; Fischr, S.; Böhm, M. C.; Lindner, H. J. *Angew. Chem., Int. Ed. Engl.* **1986**, *25*, 630.

(5) Shida, T.; Iwata, S. *J. Am. Chem. Soc.* **1973**, *95*, 3473. Carrington, A.; dos Santos-Veiga, J. *Mol. Phys.* **1962**, *5*, 21. Gerson, F.; Qin, X.-Z. *Chem. Phys. Lett.* **1988**, *153*, 546. Bock, H.; Arad, C.; Näther, C.; Havlas, Z. *J. Chem. Soc., Chem. Commun.* **1995**, 2393.

S0002-7863(97)00961-X CCC: $15.00
Published on Web 02/20/1998

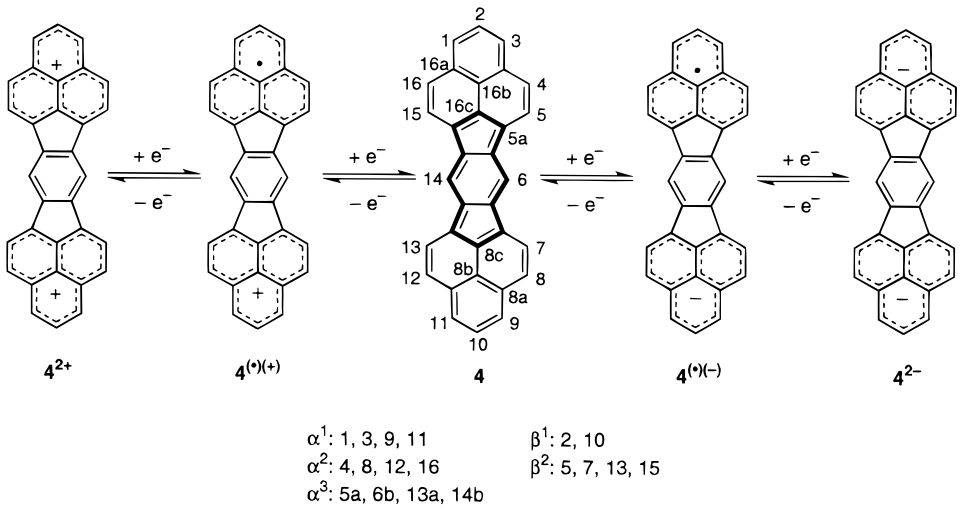

Figure 1. Four-stage amphoteric redox behavior of **4**.

compounds give even four redox species. Although unsubstituted IDPL (R = H, **4**), has been successfully isolated, its

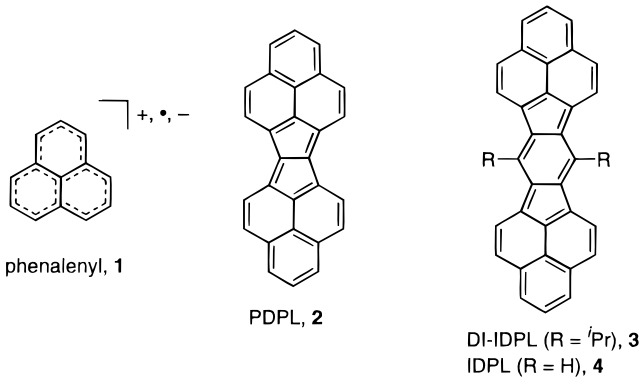

insolubility and the instability have prevented a full investigation of its properties.[6] Diisopropyl groups at C6 and C14 of **3** increase the solubility, although the redox states of **3** are not stable enough to allow for investigation of the redox properties.[1f] This forced us to introduce *tert*-butyl groups at the α-positions of the phenalenyl units in order to increase the kinetic stability and solubility. We now report the synthesis, generation, and properties of five redox states of 4,8,12,16-tetra-*tert*-butyl-*s*-indaceno[1,2,3-*cd*:5,6,7-*c′d′*]diphenalene (TTB-IDPL, **5**).

Results and Discussion

A. Synthesis. The synthetic procedure for **5** is shown in Scheme 1. A Diels−Alder reaction of **6** and **7**, followed by decarbonylation and aromatization with *p*-chloranil, afforded an isomeric mixture of the 3,10- and 3,11-dimethyl compounds **8**. Each isomer of these compounds was not isolated for further transformations because both of the isomers were expected to lead to compound **5**. Hydrolysis of the bis(ethyl ester) derivatives **8** by the conventional methods failed, but the reaction of **8** with LiI in DMF[7] successfully gave bis(carboxylic acid) compounds, which were converted to the key intermediates **9** by decarboxylation. Bis(propionic acid) derivatives **12** were obtained in three steps by the usual method. A Friedel−Crafts cyclization of the acyl chloride of **12** with $AlCl_3$ afforded the diketones **13**. The ketones **13** were reduced with $LiAlH_4$ and subsequently dehydrated with a catalytic amount of *p*-toluenesulfonic acid to afford dihydro compounds **14**. Dehydrogenation of **14** with *p*-chloranil in benzene afforded the hydrocarbon **5** as green prisms. Compound **5** was found to be stable in the solid state at room temperature.

B. Neutral State (5). Electrochemistry. The cyclic voltammogram of **5** exhibited four reversible redox waves (E_2^{ox} = +0.84 V, E_1^{ox} = +0.48 V, E_1^{red} = −0.67 V, E_2^{red} = −1.25 V; E_1^{sum} = 1.16 V, E_2^{sum} = 2.09 V), as shown in Figure 2. In contrast to DI-IDPL (**3**) giving rise to irreversible oxidation waves, **5** showed completely reversible redox waves, which provided evidence for the formation of the stable singly and doubly charged species of **5**. The small oxidation (E^{ox}) and reduction potentials (E^{red}) suggest the thermodynamic stability of the oxidized and reduced species generated, respectively. The considerably small E_1^{sum} indicates a high amphoteric-redox ability, which is consistent with the HMO calculations indicating the presence of a small HOMO−LUMO gap (0.241β) for **5**.

Crystallography. Recrystallization of **5** at room temperature gave prismatic crystals of *m*-difluorobenzene solvates. The crystal structure of **5** determined at room temperature shows an effective D_{2h} symmetry (Figure 3), which is consistent with the presence of only five ^{1}H NMR signals even at −60 °C (vide infra). In comparison with 7,14-di-*n*-propylacenaphtho[1,2-*k*]-fluoranthene (**15**),[8] **5** has a shorter bond length between C2 and C3 by 0.032−0.033 Å. This must be due, at least in part, to the increased π-bonding between C2 and C3. In the canonical forms, no double bonds appear between the naphthalene units and the central benzene unit in acenaphthofluoranthene, while **5** retains the double C2−C3 bonds. The increased π-bonding is also supported by the simple HMO calculations which indicate a larger π-bond order (0.457 for **5**; 0.402 for acenaphthofluoranthene). The large degree of π-bonding between C2 and C3 in **5** indicates that the two phenalenyl units do not function independently, but interact with each other. The strong interaction between the two phenalenyl units is also supported by the relatively large ΔE^{ox} ($E_2^{ox} - E_1^{ox}$) and ΔE^{red} ($E_1^{red} - E_2^{red}$) values discussed above.

NMR Spectroscopy. ^{1}H and ^{13}C NMR spectra of TTB-IDPL (**5**) were recorded at −30 °C. The ^{1}H and ^{13}C NMR chemical shifts are given in Table 1. Examination of the pattern of ^{1}H and ^{13}C signals indicates that **5** possesses a molecular framework

(6) Masui, T.; Yamamoto, K.; Murata, I. Unpublished results.
(7) Dean, P. D. G. *J. Chem. Soc.* **1965**, 6655.
(8) Seth, S.; Sur, H.; Chakraborty, S. *Acta Crystallogr.* **1988**, *C44*, 1011.

Scheme 1[a]

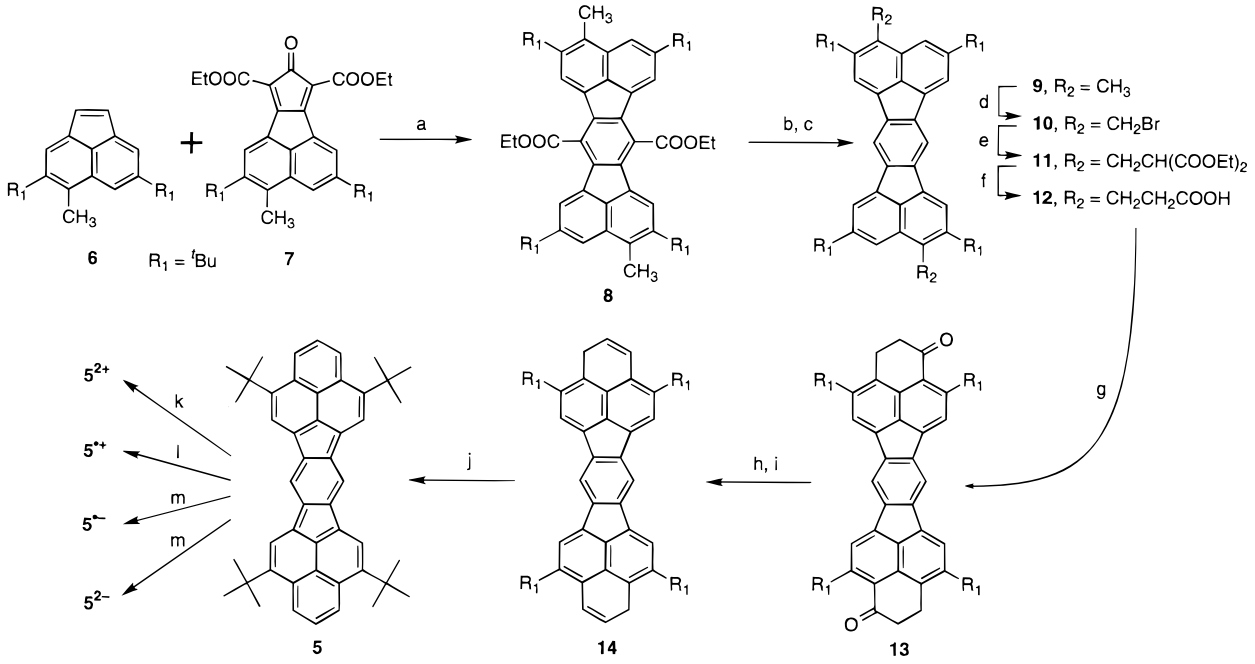

[a] Key: (a) (1) xylene, reflux, 1 h, (2) *p*-chloranil, xylene, reflux, 4 h, 99%; (b) LiI, DMF, reflux, 4 d, 99%; (c) Cu_2O, quinoline, reflux, 3 h, 95%; (d) NBS, benzoyl peroxide, benzene, reflux, 25 min; (e) NaOEt, $CH_2(CO_2Et)_2$, benzene + ethanol, rt, 3 d, 2 steps 77%; (f) (1) aqueous KOH, EtOH, (2) 4 N HCl, (3) 100 °C, 98%; (g) (1) $(COCl)_2$, (2) $AlCl_3$, CH_2Cl_2, −50 °C, 3 h, 82%; (h) $LiAlH_4$, THF, rt, 40 min, 83%; (i) cat. *p*-toluenesulfonic acid, benzene, reflux, 5 min, 81%; (j) *p*-chloranil, benzene, reflux, 40 min, 78%; (k) conc. H_2SO_4 or excess $SbCl_5$, CH_2Cl_2; (l) 1 equiv of $SbCl_5$, CH_2Cl_2; (m) K-mirror, THF, rt.

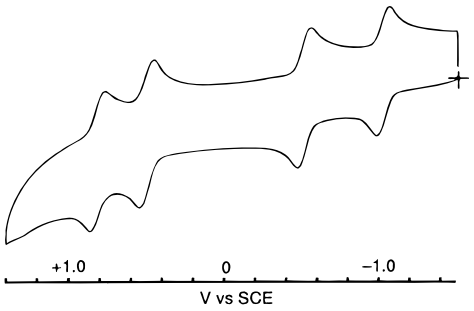

Figure 2. Cyclic voltammogram (vs SCE) of **5** in dichloromethane with 0.1 M $(^nBu)_4NClO_4$ as the supporting electrolyte at room temperature; sweep rate = 100 mv/s.

with D_{2h} symmetry, but not a localized bond structure with C_{2h} symmetry.

At elevated temperatures, progressive line broadening was observed in the ^{1}H NMR of **5** (Figure 4). The line broadening was reversible upon a temperature change of the sample solution. The ^{1}H NMR spectra of **13** and **14** exhibited sharp signals at room temperature, and furthermore, the *tert*-butyl groups of **5** gave only one sharp peak from −60 to 60 °C. These findings eliminate the possibility of broadening due to a slow rotation of the *tert*-butyl groups. Most indicative are that (1) a trace of the unidentifiable radical species was detected by ESR spectroscopy at a higher temperature than that at which the broadening of the ^{1}H NMR spectra was observed and (2) the solid **5** gave a triplet signal which increased in intensity at higher temperatures. These observations suggest two possible explanations for the behavior of the ^{1}H NMR spectra. The first is that a paramagnetic species may be present, which could easily be formed from **5** by oxidation or by the abstraction of a hydrogen atom from the solvents. Like a normal radical species, the radical species prefers the dimerization at low temperatures. At higher temperatures, the dimers dissociate to paramagnetic

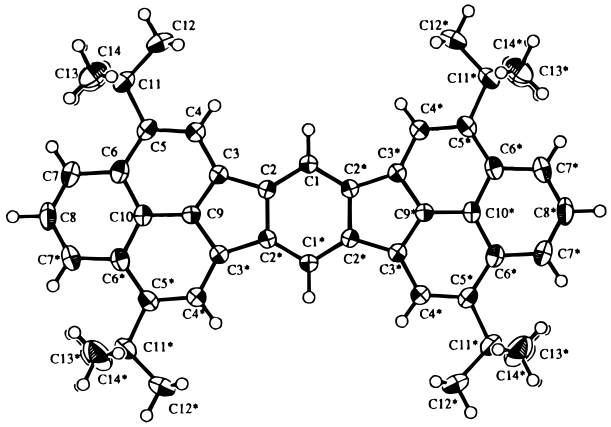

Figure 3. Molecular structure of **5** at room temperature. Displacement ellipsoids are drawn at the 50% probability level. Selected bond lengths (Å): C1−C2, 1.394(3); C2−C2*, 1.437(5); C2−C3, 1.450(4); C3−C4, 1.404(4); C3−C9, 1.399(4); C4−C5, 1.391(4); C5−C6, 1.453(4); C6−C7, 1.411(4); C6−C10, 1.433(3); C7−C8, 1.377(4); C9−C10, 1.389(5).

monomers, which cause line broadening of the NMR signals. Another explanation is that **5** can be thermally accessible to the triplet species. Most closed-shell compounds are ground-state singlets and require high energy (light absorption) for electronic excitation. However, compounds with a small HOMO−LUMO gap are able to produce the excited singlet or triplet states with a supply of low levels of energy (heat). The ground-state singlet **5** with small E_1^{sum}, i.e., a small HOMO−LUMO gap, may be in equilibrium with a thermally accessible triplet state, which causes line broadening of the NMR signals.

The ^{1}H signals at the β^2, C6, and C14 positions of **5** appear at a higher field than those of 2,5,9,12-tetra-*tert*-butylacenaphtho[1,2-*j*]fluoranthene,[9] contrasting with the lower-field shifts

Table 1. ^{1}H and ^{13}C NMR Data of **5**, $\mathbf{5}^{2+}$, and $\mathbf{5}^{2-}$

	α^1	α^2	α^3	β^1	β^2	3a,8a,11a,16a	5b,6a,13b,14a	6,14	8b,16b	8c,16c
5[a]	7.69			6.98	7.04			7.10		
$\mathbf{5}^{2+}$ [a]	8.84			7.41	7.48			6.94		
$\mathbf{5}^{2-}$ [a]	7.66			7.42	8.43			9.24		
15[a]					8.15	7.82		8.51		
5[b]	128.79	151.01	140.77	125.40	119.16	132.91	135.51	124.13	130.87	136.92
$\mathbf{5}^{2+}$ [b]	150.55	184.92	158.35	130.53	123.42	134.01	148.56	124.29	128.73	134.97
$\mathbf{5}^{2-}$ [b]	112.70	125.84	110.25	121.63	116.75	133.61	125.10	105.15	131.55	132.76

[a] ^{1}H NMR chemical shifts (δ). [b] ^{13}C NMR chemical shifts (δ): **5**, recorded in acetone-d_6 + CS_2 (1:4) at −30 °C; $\mathbf{5}^{2+}$, recorded in D_2SO_4 at room temperature; $\mathbf{5}^{2-}$, recorded in THF-d_8 at room temperature; **15**, recorded in $CDCl_3$ at room temperature.

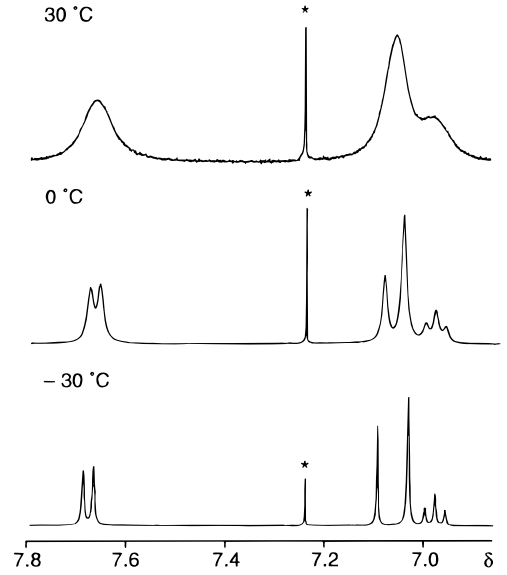

Figure 4. Temperature dependence of the ^{1}H NMR spectra of **5** in aromatic regions. A small asterisk indicates the peaks of benzene.

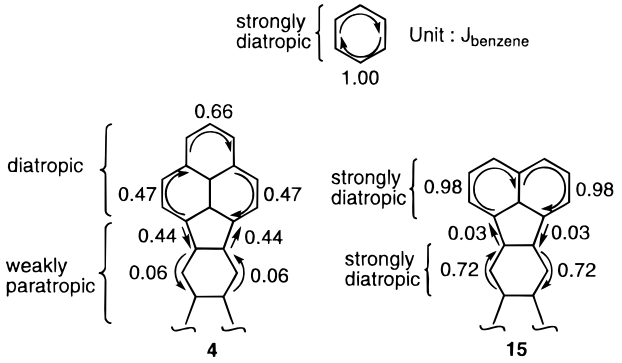

Figure 5. Ring-current calculation for **4** and **15**.

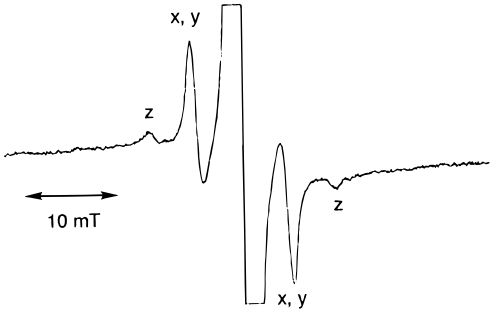

Figure 6. Triplet signal in solid state at 130 °C. The central intense peak shows the signal derived from a monoradical impurity.

of ^{13}C signals at β^2, C6, and C14. It is well established that the major effect govering the ^{13}C chemical shifts of a set of sp^2 carbons is the charge density at the relevant carbon atom. However, proton chemical shifts are sensitive to both charge-density and ring-current effects. The upfield shifts of **5** can be attributed to a paramagnetic ring-current effect. London−McWeeny ring-current calculations[10] indicate that a weakly paramagnetic ring-current is formed in the *s*-indacene unit of **5**. In contrast, a strongly diamagnetic ring current is formed in the two naphthalene and central benzene rings of **15** (Figure 5).

ESR Spectroscopy. As described above, the toluene solution of neutral **5** gave rise to weak ESR signals. The species which gave this ESR spectrum was unidentifiable, although in all likelihood it was generated by oxidation or hydrogen atom abstraction from the solvents. Although the solid **5** also gave the ESR signal (Figure 6), the spectral width was nearly 10 times larger than that observed in solution. The spectrum can be regarded as typical of a triplet state and had a zero-field parameter of $D = 9.6$ mT and $E \leq 0.2$ mT. The species to give the ESR spectrum in the solution should be a monoradical resulting from oxidation or hydrogen atom abstraction from the solvent by the reactive thermally excited triplet state. This property is characteristic of compounds with a small energy gap between the frontier orbitals. A small HOMO−LUMO gap for **5** was also indicated by the cyclic voltammogram giving a small E_1^{sum} value.

The zero-field parameter, *D*, provides a measure of the average distance between the unpaired spins in the triplet. The average distance between the two interacting spins in **5** can be estimated from *D* to be 6.6 Å,[11] which is smaller than the distance between the centers of the phenalenyl unit and the other one (9.5 Å). This suggests that an unpaired electron is not "localized" on one of the phenalenyl units, but can delocalize on the central benzene and the other phenalenyl unit. Unfortunately, the forbidden $\Delta M_s = \pm 2$ half-field absorption could not be observed. A triplet-state signal at half field is known to not be observable when there is a large separation between two electrons.[12] The variation of the signal intensity of the triplet with temperature indicates that the triplet is in a thermally excited state. A generated least-squares computer program leads

(9) ^{1}H NMR: δ 8.15 (1,6,8,13), 7.82 (3,4,10,11), 8.51 (7,14), 1.55 (^{t}Bu). ^{13}C NMR: 118.20 (1,6,8,13), 151.60 (2,5,9,12), 121.70 (3,4,10,11), 129.30 (3a,10a), 130.29 (10b,14c), 136.61 (6a,7b,13a,14b), 139.65 (6b,7a,13b,14a), 114.90 (7,14), 35.71 ($C(CH_3)_3$), 31.79 ($C(CH_3)_3$). The atom labels in parentheses are based on the IUPAC numbering system.

(10) London, F. *J. Phys. Radium* **1937**, *8*, 397. Pople, J. A. *Mol. Phys.* **1958**, *1*, 175. McWeeny, R. *Mol. Phys.* **1958**, *1*, 311. Mallion, R. B. *Mol. Phys.* **1973**, *25*, 1415. Aihara, J. *Bull. Chem. Soc. Jpn.* **1985**, *58*, 1045.

(11) D (in mT) = 2789/r^3 (in Å).

(12) de Meijere, A.; Gerson, F.; König, B.; Reiter, O.; Wellauer, T. *J. Am. Chem. Soc.* **1990**, *112*, 6827. Gerson, F.; Huber, W.; Martin, W. B., Jr.; Caluwe, P.; Pepper, T.; Szwarc, M. *Helv. Chim. Acta* **1984**, *67*, 416. Gerson, F.; Wellhause. T.; Oliver, A. M.; Paddon-Row: M. N. *Helv. Chim. Acta* **1990**, *73*, 1586. Eaton, S. S.; More, K. M.; Sawant, B. M.; Eaton, G. R. *J. Am. Chem. Soc.* **1983**, *105*, 6560.

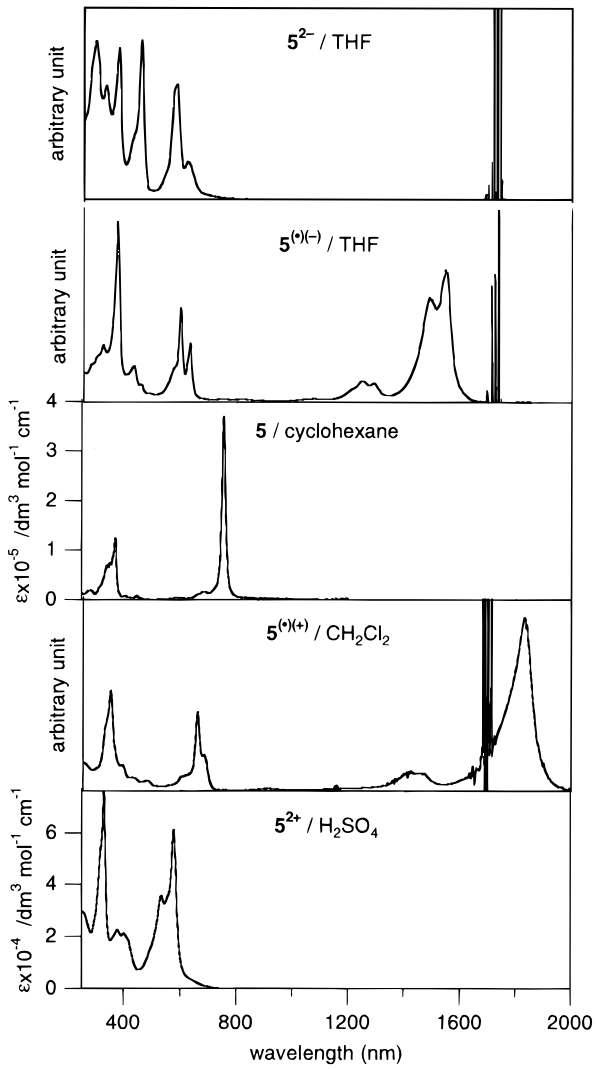

Figure 7. Electronic absorption spectra of the five redox states of **5**.

to a best fit of eq 1[13]

$$I \propto 1/\{T[3 + \exp(J/k_bT)]\} \qquad (1)$$

to the data with $J = 20.4 \pm 0.3$ kJ/mol, which is the energy separation between the ground singlet and the excited triplet states. The relatively large energy gap indicates a very small contribution from the type **5a** structure, in agreement with the double-bond character between the phenalenyl units and the central benzene ring, as mentioned in the X-ray structural analysis.

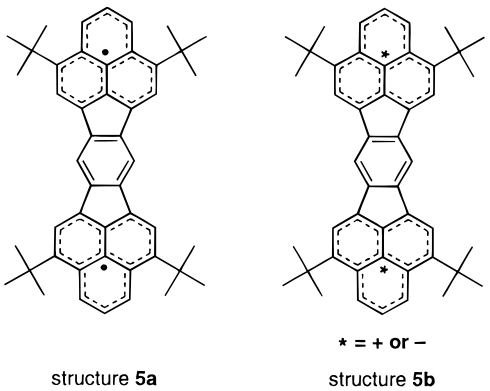

structure **5a** structure **5b**

Table 2. Maxima, λ_{max} (in nm) (ϵ, cm^{-1} M^{-1}), of Electronic Bands for the Five Redox States of **5**

5^{2+}	$5^{(\bullet)(+)}$	**5**	$5^{(\bullet)(-)}$	5^{2-}
330 (76 200)	351	342 (69 100)	320	294
378 (22 400)	393	352 (75 100)	372	330
401 (21 100)	660	370 (12 4000)	430	376
534 (35 700)	683	405 (7 900)	596	456
578 (61 200)	1440	448 (7 500)	630	582
620 (720)[a]	1832	687 (16 000)	1248	660
		755 (369 000)	1288	
			1488	
			1546	

[a] Weak shoulder peak.

Table 3. Selected Electronic Transition Data for Five Redox States of **5** Calculated by the INDO/S CI Method and Assignments of the Observed Electronic Bands

	theoretical				experimental
	symmetry label	ΔE (eV)	oscillator strength	substantial contribution (%)[a]	λ (nm); ΔE (eV)
5^{2+}	B_{2u}	1.60	0.02	a_u (ψ_{16}) ← b_{2g} (ψ_{15}), 90	*b*
$5^{(\bullet)(+)}$	B_{3u}	0.65	0.41	b_{3g} (ψ_{17}) ← a_u (ψ_{16}), 91	1832; 0.68
5	B_{3u}	1.65	2.27	b_{3g} (ψ_{17}) ← a_u (ψ_{16}), 93	755; 1.64
$5^{(\bullet)(-)}$	B_{3u}	0.73	0.32	b_{3g} (ψ_{17}) ← a_u (ψ_{16}), 84 a_u (ψ_{18}) ← b_{3g} (ψ_{17}), 6	1546; 0.80
5^{2-}	B_{3u}	2.44	1.37	a_u (ψ_{18}) ← b_{3g} (ψ_{17}), 84 b_{3g} (ψ_{20}) ← a_u (ψ_{16}), 10	660; 1.88

[a] In parentheses, the molecular orbitals calculated by the HMO method. See Figure 9. [b] Could not be assigned due to the weak and broad peaks.

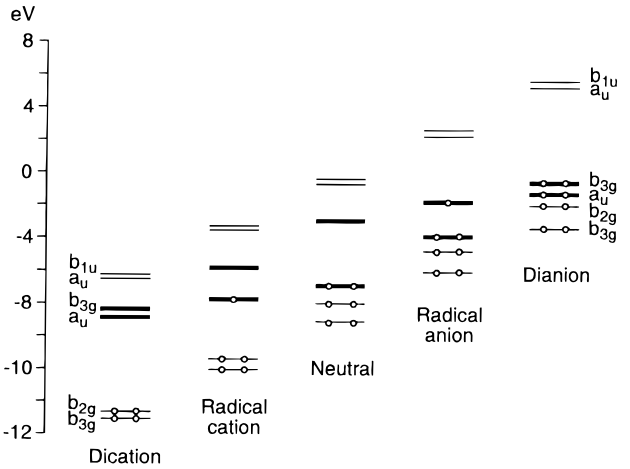

Figure 8. Energy levels of several occupied and unoccupied MOs in the five redox stages of IDPL **4**, as calculated by the MOPAC6/PM3 method. The optimized structures are in D_{2h} symmetry for all states. The bold lines represent the HOMO and LUMO of the neutral state.

UV−Vis−Near-IR. Although all precursors for TTB-IDPL (**5**) were a yellow color, dehydrogenation of the dihydro derivatives **14** caused a dramatic change in color; the solution of **5** shows a green color. Figure 7 shows the electronic absorption spectra of the five redox states of **5**, and Table 2 lists the wavelengths of the band maxima.

The green color of **5** can be reasonably ascribed to a highly intense band at 755 nm. To assign the electronic absorption bands to transitions between orbitals, MO calculations by the INDO/S CI method were performed (Table 3). In each case, the 10 highest occupied and 10 lowest unoccupied orbitals were used for configuration interactions. Figure 8 schematically presents the calculated SCF energy levels of the six relevant

(13) Bleaney, B.; Bowers, K. D. *Proc. R. Soc. London Ser. A* **1952**, 214. Bijl, D.; Kainer, H.; Rose-Innes, A. C. *J. Chem. Phys.* **1959**, *30*, 765.

highest occupied or lowest unoccupied orbitals for the five redox states of **5**. On the basis of the calculations, the intense band at 755 nm can be assigned to a symmetry-allowed B_{3u} transition, which corresponds to a HOMO → LUMO excitation. Thus, the electronic absorption spectrum of the neutral state reflects the small HOMO−LUMO gap of **5**.

Charge-Transfer Complex. The neutral hydrocarbon **5** with the small E_1^{ox} and E_1^{red} is expected to behave as both a donor and an acceptor. Although **5** has unfortunately given no CT complex with donors so far, **5** was found to form a CT complex with acceptors. The 1:1 complex formed between 7,7,8,8-tetracyanoquinodimethane (TCNQ), and **5** crystallized as deep green needles by recrystallization from a CH_2Cl_2 solution at 5 °C. The crystal structure consists of infinite columns of alternate TCNQ and **5** molecules stacked in a plane-to-plane manner in columns along the *c* axis of the unit cell. A TCNQ molecule lies on the phenalenyl unit corresponding to the redox site of **5**, with an interplanar distance of 3.33 Å between TCNQ and the rings of **5**. The bond lengths and angles of **5** and TCNQ are found to be similar to those of neutral **5** and neutral TCNQ,[14] respectively.

The degree of charge transfer for TCNQ complexes can be estimated from the ratio $c/(b + d)$.[15]

The application of this equation to the **5**·TCNQ complex gives a value of 0.474, which is identical to that of neutral TCNQ. The frequency of the CN stretching mode can also provide an estimate of the charge on TCNQ.[16] The IR spectra of the **5**·TCNQ complex exhibited a peak at 2214 cm^{-1}, from which the charge on TCNQ could be estimated to be about 0.3. The electronic absorption spectra of the complex gave intense peaks at 790 and 364 nm, which were assignable to local $\pi-\pi^*$ transitions of neutral **5**. In addition to these intense bands, weak charge-transfer bands were observed in 1200−2600 nm. In a CH_2Cl_2 solution of the complex, no charge-transfer bands could be observed. The weak charge-transfer interaction suggests that each component of the molecules in the complex retain a similar structure to that of the neutral state. Thus, the ground state of the complex should be nearly neutral.

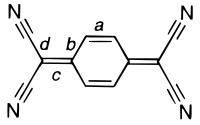

C. Radical Cation ($5^{(\bullet)(+)}$) and Radical Anion ($5^{(\bullet)(-)}$). ESR Spectroscopy. The low first oxidation potential (E_1^{ox}) and the high first reduction potential (E_1^{red}) indicate that TTB-IDPL (**5**) should be easily oxidized to the radical cation $\mathbf{5}^{(\bullet)(+)}$ and reduced to the radical anion $\mathbf{5}^{(\bullet)(-)}$. Furthermore, the reversible redox waves in the cyclic voltammogram for **5** suggest that both of the radical species are stable. The reaction of **5** with $SbCl_5$ in CH_2Cl_2 generated the radical cation $\mathbf{5}^{(\bullet)(+)}$, which was found to be stable at room temperature and gave rise to the well-resolved ESR spectrum. No detectable changes were observed in the spectra in the range of 213−273 K. The coupling constants of the ring protons are given in Table 4 along with the theoretical coupling constants calculated by the HMO−McLachlan method ($\lambda = 1.2$)[17] and McConnell equation ($Q = -2.4$ mT).[18] The assignment of the coupling constants is based on the calculated spin density and is confirmed by studies of the radical cation of the 2,10-dideuterated derivative.

Table 4. Experimental and Theoretical Hyperfine Coupling Constants (in mT) of $\mathbf{5}^{(\bullet)(+)}$ and $\mathbf{5}^{(\bullet)(-)}$

	$\mathbf{5}^{(\bullet)(+)a}$		$\mathbf{5}^{(\bullet)(-)b}$	
	experimental	theoretical[c]	experimental	theoretical[c]
α^1	0.250	0.251	0.240	0.249
β^1	0.0725	−0.0752	0.0732	−0.0729
β^2	0.0375	−0.0118	0.0905	−0.0799
6,14	0.0463	−0.0494	0.240	0.235

[a] Recorded in CH_2Cl_2 at −20 °C. The *g*-value was 2.0025. [b] Recorded in THF at −20 °C. The *g*-value was 2.0024. [c] Calculated by the HMO−McLachlan method ($\lambda = 1.2$) and the McConnell equation ($Q = -2.4$ mT).

The radical anion $\mathbf{5}^{(\bullet)(-)}$ was obtained by the treatment of **5** with a potassium mirror in THF. The radical anion was also stable and gave rise to the well-resolved ESR spectrum. No detectable changes were observed in the spectrum in the range of 213−273 K. Table 4 shows the experimental and the theoretical hyperfine coupling (hfc) constants of $\mathbf{5}^{(\bullet)(-)}$.

The agreement between the four sets of hfc constants and the theoretical values indicates that the unpaired electron is not confined to one limited phenalenyl unit but is delocalized over the entire molecule in $\mathbf{5}^{(\bullet)(+)}$ and $\mathbf{5}^{(\bullet)(-)}$. The highly delocalized structure is supported by the HMO−McLachlan calculations, which indicate that 86% of the π-spin population resides on the two phenalenyl units in both the radical species.

The π-spin distribution of $\mathbf{5}^{(\bullet)(-)}$ should relate closely to the π-charge distribution of the dianion $\mathbf{5}^{2-}$, because the unpaired electron in $\mathbf{5}^{(\bullet)(-)}$ occupies, in principle, the same orbital (LUMO of **5**) as the two paired electrons in $\mathbf{5}^{2-}$. An analogous statement holds for the π-spin distribution in the radical cation $\mathbf{5}^{(\bullet)(+)}$ and the π-charge distribution in $\mathbf{5}^{2+}$. Comparison of the coupling constants of $\mathbf{5}^{(\bullet)(-)}$ with ^{13}C chemical shift changes on going from **5** to $\mathbf{5}^{2-}$ (vide infra) shows a good correlation, indicating that these values are large at $C^{\alpha 1}$, C6, and C14, and small at $C^{\beta 1}$ and $C^{\beta 2}$. For $\mathbf{5}^{(\bullet)(+)}$ and $\mathbf{5}^{2+}$, large coupling constants and chemical shift changes are found at $C^{\alpha 1}$ and small ones at $C^{\beta 1}$, $C^{\beta 2}$, C6, and C14. Consequently, both the radical species exhibit larger coupling constants at $C^{\alpha 1}$ than those at $C^{\beta 1}$ and $C^{\beta 2}$ in the two phenalenyl units. Such a π-spin distribution pattern can be found in phenalenyl radical species exhibiting larger (0.65 mT) and smaller (0.18 mT) coupling constants at the α and β positions, respectively.[3b] Furthermore, as shown below, the charge distributions in phenalenyl units of $\mathbf{5}^{2+}$ are similar to those of phenalenyl cation. These similarities support the idea that the HOMO of **5** to some extent retains an NBMO character. On the other hand, the LUMO of **5** should have a pure NBMO character on the basis of the HMO calculation (Figure 9). Thus, the small E_1^{sum} value of **5** can be attributed to the NBMO character of the frontier orbitals (HOMO and LUMO) of **5**.

UV−Vis−Near-IR. Oxidation or reduction of aromatic hydrocarbons such as naphthalene and anthracene results in the formation of a deeply colored solution. The following statements would be expected to be true on the basis of this observation. The species responsible for these colors are undoubtedly radical ions. Additional long-wavelength bands, which are not observed for the neutral aromatic compounds, are due to the transition in which a singly occupied MO (SOMO) participates; SOMO → LUMO, HOMO → SOMO excitation, etc. However, when green compound **5** was oxidized or reduced

(14) Dunitz, J. D.; Krüger, C.; Irngartinger, H.; Maverick, E. F.; Wang, Y.; Nixdorf, M. *Angew. Chem., Int. Ed. Engl.* **1988**, *27*, 387.
(15) Kistenmacher, T. J.; Emge, T. J.; Bloch, A. N.; Cowan, D. O. *Acta Crystallogr.* **1982**, *B38*, 1193.
(16) Chappell, J. S.; Bloch, A. N.; Bryden, W. A.; Maxfield, M.; Poehler, T. O.; Cowan, D. O. *J. Am. Chem. Soc.* **1981**, *103*, 2442.
(17) McLachlan, A. D. *Mol. Phys.* **1960**, *3*, 233.
(18) McConnell, H. M. *J. Chem. Phys.* **1956**, *24*, 764.

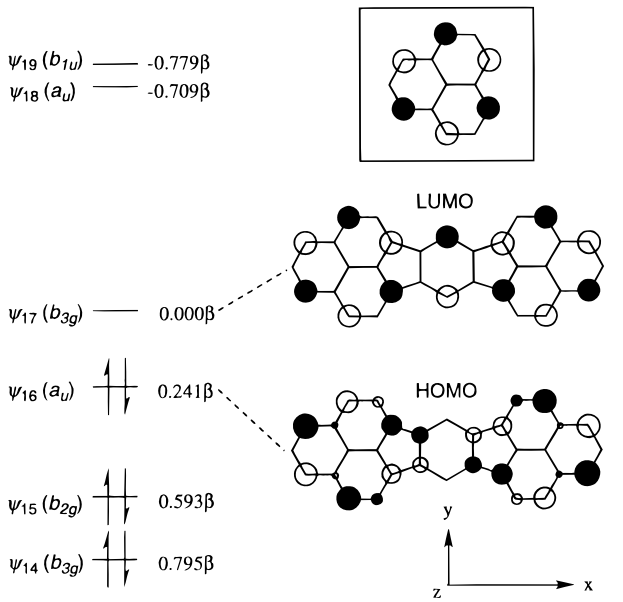

Figure 9. Selected molecular orbitals of **4** calculated by the HMO method. The insert gives the NBMO of the phenalenyl radical.

with $SbCl_5$ or K-mirror, the color of the solution did not change dramatically. The resulting green and greenish blue color of the solution containing $\mathbf{5}^{(\bullet)(+)}$ and $\mathbf{5}^{(\bullet)(-)}$ can be reasonably attributed to absorption bands at $\lambda \leq 683$ and 630 nm, respectively. In addition to these long-wavelength absorptions, $\mathbf{5}^{(\bullet)(+)}$ and $\mathbf{5}^{(\bullet)(-)}$ gave lower energy bands in the near-infrared (near-IR) region (Figure 7). The INDO/S calculations indicate that the near-IR bands of $\mathbf{5}^{(\bullet)(+)}$ and $\mathbf{5}^{(\bullet)(-)}$ should be due to the excited configuration corresponding to b_{3g} (ψ_{17}) ← a_u (ψ_{16}) excitation (symmetry-allowed B_{3u} transition), which is SOMO → LUMO excitation for $\mathbf{5}^{(\bullet)(+)}$ and HOMO → SOMO for $\mathbf{5}^{(\bullet)(-)}$ (Table 3). These low-energy transitions in the near-IR region imply a small HOMO-LUMO gap of **5** because the MO ψ_{16} and ψ_{17} correspond to the HOMO and the LUMO for **5**, respectively. Such long-wavelength absorptions of radical ions can be observed in some aromatic compounds. For example, a green-colored neutral hydrocarbon, hexacene, gives a near-IR band in the radical anion state due to the HOMO → SOMO excitation.[19]

D. Dication (5^{2+}) and dianion (5^{2-}). NMR Spectroscopy: Dication. The dication species $\mathbf{5}^{2+}$ was obtained as a purple solution, by dissolving **5** in concentrated D_2SO_4, or as purple needles, by treating **5** with excess $SbCl_5$ in dichloromethane. The ^1H and ^{13}C NMR chemical shifts are given in Table 1.

The total ^{13}C chemical shift change ($\Sigma\Delta\delta c$) of the sp^2 carbons on going from **5** to $\mathbf{5}^{2+}$ is 369 or 185 ppm per electron. This value is in good agreement with the Spiesecke and Schneider correlation predicting a total ^{13}C chemical shift of 160−200 ppm per unit charge.[20] A comparison of the ^{13}C NMR signals of the two phenalenyl units of $\mathbf{5}^{2+}$ with those of the phenalenyl cation species[3d] reveals only minor differences in the chemical shifts for equivalent carbon atoms, except for the α^2 carbons of $\mathbf{5}^{2+}$ deshielded by the *tert*-butyl groups. This indicates that the positive charge is delocalized mainly over two phenalenyl units, with a charge distribution similar to that of the phenalenyl cation species, in accordance with HMO calculations which give a total charge density of +1.82 on two phenalenyl units. However, $H^{\alpha 1}$, $H^{\beta 1}$, and $H^{\beta 2}$ of $\mathbf{5}^{2+}$ are more shielded than the protons of the phenalenyl cation species. The upfield shifts can be related to the formation of a paramagnetic ring-current effect. On the basis of the ring-current calculations on the parent species $\mathbf{4}^{2+}$ (Figure 10), $\mathbf{5}^{2+}$ should show strong and weak paratropism at the central *s*-indacene and the terminal benzene rings, respectively.

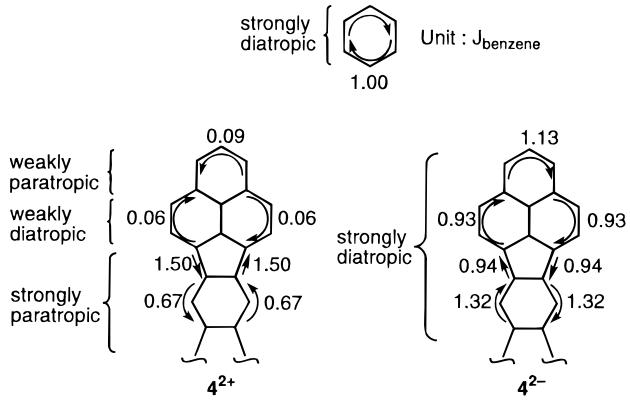

Figure 10. Ring-current calculation of $\mathbf{4}^{2+}$ and $\mathbf{4}^{2-}$.

NMR Spectroscopy: Dianion. Treatment of dihydro compounds **14** with a potassium mirror in a sealed degassed tube at −78 °C yielded the dianion species $\mathbf{5}^{2-}$ as a deep blue solution. The ^1H and ^{13}C NMR chemical shifts are given in Table 1.

The ^{13}C NMR spectrum of the dianion $\mathbf{5}^{2-}$ reveals reasonably a dianionic nature with a total upfield shift of 388 ppm. The ^{13}C chemical shifts for the sp^2 carbons change largely at the α1, α2, α3, C6, and C14 positions, but change only slightly at other positions, on going from **5** to $\mathbf{5}^{2-}$. This result is consistent with the NBMO character of the LUMO of **5**, which possesses coefficients of +0.071 or −0.071 at the α1, α2, α3, C6, and C14 positions and of zero at other positions (Figure 9). Despite the shielding effect of the negative charges, all protons appear considerably far into the downfield region. In particular, the largest downfield shift is observed in H6 and H14, although C6 and C14 signals appear in the highest field among the sp^2 carbons of $\mathbf{5}^{2-}$. The upfield shifts of ^{13}C signals, at C6 and C14, and HMO calculations reveal that the charge densities at C6 and C14 are more negative in $\mathbf{5}^{2-}$ than those in **5**. These findings suggest that the opposite effect of the diamagnetic deshielding relative to the shielding due to the negative charges is even more significant for the ^1H chemical shifts in $\mathbf{5}^{2-}$. The ring-current calculations indicate that a strongly diamagnetic ring current will be formed along the periphery of $\mathbf{5}^{2-}$, with the contribution of a peripheral 28C-30π conjugate system[21] (Figure 10).

Both dication and dianion species are stable at room temperature. On the basis of the HMO calculation, two phenalenyl units have 91% of the total positive charges and 86% of the total negative charges in the dication and dianion states, respectively. This reflects the large contribution of the type **5b** structure to the stability of both doubly charged species.

UV−Vis−Near-IR. The absorption maxima of $\mathbf{5}^{2+}$ and $\mathbf{5}^{2-}$ appear at a shorter wavelength than those of the other redox states of **5**. In particular, the absorption of $\mathbf{5}^{2-}$ terminates at the shortest wavelength. This finding suggests the presence of a large HOMO−LUMO gap for $\mathbf{5}^{2-}$, which is consistent with the HMO calculations. Because a large HOMO−LUMO gap contributes a small of a paramagnetic ring-current effect to the

(19) Angliker, H.; Gerson, F.; Lopez, J.; Wirz, J. *Chem. Phys. Lett.* **1981**, *81*, 242. Angliker, H.; Rommel, E.; Wirz, J. *Chem. Phys. Lett.* **1982**, *87*, 208.

(20) Spiesecke, H.; Schneider, W. G. *Tetrahedron Lett.* **1961**, 468.

(21) Another peripheral 28C-30π system is diindenoperylene dianion. See: Minsky, A.; Rabinovitz, M. *Tetrahedron Lett.* **1981**, *22*, 5341.

molecule in question, the hypsochromic shifts of $\mathbf{5}^{2-}$ support the idea that the low-field shifts of the ^{1}H NMR spectrum for $\mathbf{5}^{2-}$ are caused by a strong diamagnetic ring-current effect.

The assignment of the first absorption bands in $\mathbf{5}^{2+}$ and $\mathbf{5}^{2-}$ remains questionable. For $\mathbf{5}^{2+}$, a weak transition was observed at 620−720 nm, but the absorption maxima could not be determined due to the broad and weak absorptions. The INDO/S calculations predict the symmetry-forbidden HOMO−LUMO transition at 775 nm, which may correspond to the absorption at 620−720 nm.

Conclusion

As expected, TTB-IDPL (**5**) was found to behave as a four-stage amphoteric redox compound. The X-ray structural analysis revealed that **5** had a delocalized structure with a D_{2h} symmetry. The ^{13}C NMR and ESR spectra suggested that the charges and the spin of four charged species of **5** were delocalized over the whole of the molecules and were distributed on the two phenalenyl units of **5**, similar to phenalenyl species. The similarity of the distribution pattern supports the NBMO character for the HOMO and LUMO of **5**. The NBMO character of the frontier orbitals could be responsible for the small HOMO−LUMO gap, i.e., the small E_1^{sum} value, which is consistent with the low-energy transition at 755 nm observed in the UV−vis−near-IR spectrum of neutral **5**. In conclusion, phenalenyl units strongly contribute to the higher amphotericity of **5** and the stability of the redox species generated.

Experimental Section

Material and Methods. All experiments with moisture- or air-sensitive compounds were performed in anhydrous solvents under an argon atmosphere in flame-dried glassware. Solvents were dried and distilled according to the standard procedures. Column chromatography were performed with silica gel [Wako gel C-200 (Wako)] or basic alumina [200 mesh (Wako)]. Infrared spectra were recorded on a Perkin-Elmer FT 1640 IR spectrometer. Electronic spectra were measured by a Shimadzu UV-3100PC spectrometer. ^{1}H and ^{13}C NMR spectra were obtained on JEOL EX-270, JEOL GSX-400, JEOL GSX-500, and Varian UNITY plus 600 spectrometers. Positive EI, FAB, and FD mass spectra were taken by using JEOL JMS SX-102 and Shimadzu QP-5000 mass spectrometers. ESR spectra were obtained with a JEOL JES-FE2XG spectrometer. Cyclic voltammetric measurements were made with a Yanagimoto P1100 spectrometer. Cyclic voltammograms of the compounds were recorded with glassy carbon working electrode and Pt counter electrode in CH_2Cl_2 containing 0.1 M $(n\text{-Bu})_4NClO_4$ as the supporting electrolyte. The experiments employed a SCE reference electrode. Electrochemical experiments were done under an argon atmosphere at room temperature.

X-ray Crystallography. X-ray structure determination of **5** ($C_{60}H_{54}F_4$, MW = 851.08): crystal dimensions 0.20 × 0.30 × 0.30 mm^3, green, Rigaku AFC7R diffractometer, Mo Kα radiation, T = 296 K, orthorhombic, a = 32.602(3), b = 11.768(3), and c = 12.199(3) Å, V = 4680(2) Å^3, Z = 4, d_{cell} = 1.208 Mg/m^3, space group C_{mca}, 3002 reflections measured, 1163 reflections observed ($I > 3.00\ \sigma(I)$), $2\theta_{max}$ = 55.0°, structure solution with direct methods (MITHRIL 90) and refinement on F with 174 parameters, R = 0.054, R_w = 0.057, S = 2.14. For **5**·TCNQ complex ($C_{62}H_{56}N_4Cl_4$, MW = 998.96): crystal dimensions 0.20 × 0.10 × 0.10 mm^3, green, R-Axis CS diffractometer, Mo Kα radiation, T = 288 K, triclinic, a = 32.602(3), b = 11.768(3), and c = 12.199(3) Å, α = 103.12(2)°, β = 112.18(1)°, γ = 69.02(2)°, V = 1354(6) Å^3, Z = 1, d_{cell} = 1.225 Mg/m^3, space group $P\bar{1}$, 2745 reflections measured, 2736 reflections observed ($I > 3.00\ \sigma(I)$), $2\theta_{max}$ = 59.7°, structure solution with direct methods (MULTAN88), and refinement on F with 174 parameters, R = 0.102, R_w = 0.105, S = 2.84.

4,7-Di-*tert*-butyl-5-methylacenaphthylene (6). To a refluxing solution of di-*tert*-butylmethylacenaphthenol (201 mg, 678 mmol) in benzene (70 mL) was added *p*-toluenesulfonic acid monohydrate (15 mg), and the reaction mixture was stirred for 20 min. The mixture was cooled on an ice-bath, washed with saturated aqueous $NaHCO_3$ and brine, dried over $MgSO_4$, and filtered. After evaporation of the solvent, the crude product was purified by column chromatography on silica gel (hexane) to give **6** (172 mg, 91%) as yellow oil: ^{1}H NMR (270 MHz, $CDCl_3$) δ 7.98 (d, J = 1.0 Hz, 1H), 7.76 (s, 1H), 7.73 (d, J = 1.0 Hz, 1H), 6.98 (d, J = 5.1 Hz, 1H), 6.93 (d, J = 5.1 Hz, 1H), 2.97 (s, 3H), 1.53 (s, 9H), 1.45 (s, 9H); EI MS m/z 278 (M^+).

Diethyl 2,5-Di-*tert*-butyl-3-methyl-8-oxocyclopenta[*a*]acenaphthylene-7,9-dicaboxylate (7). Diethyl 1,3-acetonedicarboxylate (2.9 mL, 16.0 mmol) was added to a suspension of 4,7-di-*tert*-butyl-5-methylacenaphthenequinone (4.51 g, 14.6 mmol) in 55 mL of THF. A methanol solution (40 mL) of triethylamine (2.45 mL, 17.6 mmol) was added dropwise over 5 min to the mixture. The mixture was stirred for 12 h at room temperature and poured into a mixture of benzene (250 mL) and 2 N hydrochloric acid (30 mL). The organic layer was separated, washed with brine, dried over $MgSO_4$, and filtered. Purification of the crude product by column chromatography on silica gel (dichloromethane), and subsequent recrystallization from dichloromethane afforded compound **7** as purple needles: mp 222.0−224.5 °C (dec.); ^{1}H NMR (270 MHz, $CDCl_3$) δ 8.84 (s, 1H), 8.72 (d, J = 1.3 Hz, 1H); 8.15 (d, J = 1.3 Hz, 1H), 4.46 (q, J = 7.2 Hz, 4H), 2.98 (s, 3H), 1.62 (s, 9H), 1.51 (s, 9H), 1.48 (t, J = 7.2 Hz, 3H), 1.45 (t, J = 7.2 Hz, 3H); FAB MS (NBA) m/z 474 (M^+); IR (KBr) 2979, 2953, 1741, 1725, 1693, 1652, 1631, 1608 cm^{-1}. Anal. Calcd for $C_{30}H_{34}O_5$: C, 75.92; H, 7.22. Found: C, 75.94; H, 7.21.

Diethyl 2,5,9,12-Tetra-*tert*-butyl-3,10/11-dimethylacenaphtho[1,2-*k*]fluoranthene-7,14-dicarboxylate (8). A mixture of **6** (848 mg, 3.05 mmol) and **7** (948 mg, 2.0 mmol) in 35 mL of xylenes was refluxed. After 80 min, *p*-chloranil (565 mg, 1 mmol) was added, and the mixture was refluxed for an additional 3.5 h. The reaction mixture was cooled and concentrated in vacuo. The crude product was purified by column chromatography on alumina (benzene) to give **8** (1.43 g, 99%) as yellow powder: mp > 300 °C; ^{1}H NMR (270 MHz, $CDCl_3$) δ 8.07 (br s, 4H), 8.06 (br s, 2H), 4.78, 4.76, 4.74 (q, q, q, J = 7.2 Hz, 4H), 3.02 (s, 3H), 1.61 (s, 18H), 1.52 (s, 18H), 1.57, 1.55, 1.53 (t, t, t, J = 7.2 Hz, 6H); FD MS m/z 722 (M^+). Anal. Calcd for $C_{50}H_{58}O_4$: C, 83.06; H, 8.09. Found: C, 83.22, H, 8.14.

2,5,9,12-Tetra-*tert*-butyl-3,10/11-dimethylacenaphtho[1,2-*k*]-fluoranthene (9). A suspension of compound **8** (3.30 g, 4.56 mmol) and LiI (19.0 g, 142 mmol) in 150 mL of DMF was refluxed for 4 days. The reaction mixture was cooled and poured into 2 N hydrochloric acid (250 mL). The resulting yellow precipitate was filtered off, washed with water, and dried to yield 3.00 g (99%) of the dicarboxylic acid: ^{1}H NMR (270 MHz, acetone-d_6) δ 8.43 (s, 2H), 8.37 (d, J = 1.0 Hz, 2H), 3.21 (d, J = 1.0 Hz, 2H), 3.06 (s, 6H), 1.63 (s, 18H), 1.54 (s, 18H).

A suspension of the crude dicarboxylic acid (1.26 g, 1.89 mmol) and Cu_2O (254 mg, 1.77 mmol) in 40 mL of quinoline was refluxed for 3 h. The reaction mixture was cooled and poured into 2 N hydrochloric acid (200 mL). Dichloromethane was added to the mixture, and the organic layer was separated. The aqueous layer was extracted repeatedly with a small amount of dichloromethane. The combined organic layers were dried over Na_2SO_4 and filtered. The crude product was purified by column chromatography on silica gel [benzene/hexane (1:4, v/v)] to give **9** (1.09 g, 95%) as yellow powder: mp > 300 °C; ^{1}H NMR (270 MHz, $CDCl_3$) δ 8.44, 8.39, 8.36 (s, s, s, 2H), 8.14 (s, 2H), 8.10 (d, J = 1.3 Hz, 2H), 8.01 (d, J = 1.3 Hz, 2H), 3.02 (s, 6H), 1.64 (s, 18H), 1.54 (s, 18H); FAB MS (NBA) m/z 578 (M^+). Anal. Calcd for $C_{44}H_{50}$: C, 91.29; H, 8.71. Found: C, 90.97; H, 8.67.

2,5,9,12-Tetra-*tert*-butyl-3,10/11-bis(bromomethyl)acenaphtho-[1,2-*k*]fluoranthene (10). A mixture of compound **9** (966 mg, 1.67 mmol), *N*-bromosuccinimide (663 mg, 3.67 mmol), and benzoyl peroxide (88.5 mg, 0.365 mmol) in 120 mL of benzene was refluxed for 25 min. The reaction mixture was cooled and concentrated in vacuo. The resulting orange powder was washed with ethanol repeatedly to give crude **10**: ^{1}H NMR (270 MHz, $CDCl_3$) δ 8.38, 8.36, 8.33 (s, s, s,

2H), 8.19 (s, 2H), 8.09 (s, 2H), 8.08 (s, 2H), 5.46 (s, 4H), 1.69 (s, 18H), 1.56 (s, 18H); FD MS *m*/*z* 734, 736, 738 (M^+).

2,5,9,12-Tetra-*tert*-butyl-3,10/11-bis[2,2-bis(ethoxycarbonyl) ethyl]acenaphtho[1,2-*k*]fluoranthene (11). Diethyl malonate (4.3 mL, 28.3 mmol) was added to a sodium ethoxide solution freshly prepared from 37 mL of anhydrous ethanol and sodium (628 mg, 27.3 mmol). To the clear solution was added **10** suspended in benzene (120 mL). After 18 h of stirring, the reaction mixture was washed with water. The organic layer was separated, and the aqueous layer was extracted repeatedly with benzene. The combined organic layers were dried over $MgSO_4$ and filtered. After evaporation of the solvent, the crude product was purified by column chromatography on silica gel (benzene) to give **11** (1.12 g, 77%, 2 steps) as yellow powder: mp 260.5−266.0 °C (dec.); ^{1}H NMR (270 MHz, $CDCl_3$) δ 8.43, 8.40, 8.36 (s, s, s, 2H), 8.17 (d, J = 1.0 Hz, 2H), 8.16 (s, 2H), 8.08 (br s, 2H), 4.20 (d, J = 6.9 Hz, 4H), 4.12, 4.08, 3.99, 3.95 (q, q, q, q, J = 7.3 Hz, 8H), 3.80 (t, J = 6.9 Hz, 2H), 1.63 (s, 18H), 1.52 (s, 18H), 1.03 (t, J = 7.3 Hz, 12H); FAB MS (NBA) *m*/*z* 894 (M^+); IR (KBr) 2959, 1752, 1729 cm^{-1}. Anal. Calcd for $C_{58}H_{70}O_8$: C, 77.82; H, 7.88. Found: C, 78.22; H, 7.93.

2,5,9,12-Tetra-*tert*-butyl-3,10/11-bis(2-carboxyethyl)acenaphtho-[1,2-*k*]fluoranthene (12). A suspension of **11** (1.13 g, 1.26 mmol) in ethanol (200 mL) and 10% aqueous potassium hydroxide solution (100 mL) was refluxed for 20 h. The reaction mixture was cooled and concentrated in vacuo. A suspension of the obtained yellow solid in 1 N hydrochloric acid (400 mL) was heated to reflux for 84 h. The resulting yellow precipitate was collected and washed with water to give crude **12** (856 mg, 98%): IR (KBr) 3440, 1706 cm^{-1}.

4,8,12,16-Tetra-*tert*-butyl-1,2,3,9,10,11-hexahydro-1,9/11-dioxo-*s*-indaceno[1,2,3-*cd*:5,6,7-*c*′*d*′]diphenalene (13). A mixture of compound **12** (510 mg, 734 mmol) and oxalyl chloride (2 mL, 23 mmol) in benzene (200 mL) was heated to reflux for 2 h. The reaction mixture was cooled and concentrated in vacuo. The resulting orange solid dissolved in dichloromethane (200 mL) was cooled to −78 °C. Anhydrous $AlCl_3$ (1.35 g, 10.1 mmol) was added to the solution, and the reaction mixture was allowed to warm to −50 °C over 2 h and stirred at −50 °C for 3 h. Hydrochloric acid (2 N) was added to the mixture, and the organic layer was separated. The aqueous layer was extracted with dichloromethane. The combined organic layers were washed with brine, dried over Na_2SO_4, and filtered. After column chromatography on silica gel (benzene), pure **13** (397 mg, 82%) was obtained as an orange powder: mp > 300 °C; ^{1}H NMR (270 MHz, $CDCl_3$) δ 8.48, 8.44, 8.41 (s, s, s, 2H), 8.33, 8.32 (s, s, 2H), 8.21, 8.20 (s, s, 2H), 3.85 (t, J = 6.8 Hz, 4H), 3.15 (t, J = 6.8 Hz, 2H), 1.67 (s, 18H), 1.64 (s, 18H); FAB MS (NBA) *m*/*z* 659 (M^+ + H); IR (KBr) 2962, 2912, 1696 cm^{-1}. Anal. Calcd for $C_{48}H_{50}O_2$: C, 87.49; H, 7.65. Found: C, 87.29; H, 7.60.

4,8,12,16-Tetra-*tert*-butyl-1,2,3,9,10,11-hexahydro-1,9/11-dihydroxy-*s*-indaceno[1,2,3-*cd*:5,6,7-*c*′*d*′]diphenalene. A mixture of **13** (126 mg, 191 mmol) and lithium aluminum hydride (13 mg, 343 mmol) in THF (60 mL) was stirred for 20 min at room temperature. After addition of dichloromethane, the mixture was washed with brine. The organic layer was separated and the aqueous layer was extracted repeatedly with dichloromethane. The combined organic layers were dried over Na_2SO_4 and filtered. After column chromatography on silica gel (dichloromethane), pure diol (106 mg, 83%) was obtained as yellow powder: ^{1}H NMR (270 MHz, $CDCl_3$) δ 8.39, 8.38, 8.37 (s, s, s, 2H), 8.20 (s, 2H), 8.19 (s, 2H), 5.85 (m, 2H), 3.66 (m, 2H), 3.49 (m, 2H), 2.56 (m, 2H), 2.19 (m, 2H), 1.72 (s, 18H), 1.67 (s, 18H); FAB MS (NBA) *m*/*z* 662 (M^+); IR (KBr) 3425, 2954 cm^{-1}.

4,8,12,16-Tetra-*tert*-butyl-1,9/11-dihydro-*s*-indaceno[1,2,3-*cd*:5,6,7-*c*′*d*′]diphenalene (14). Diols (54.1 mg, 81.6 mmol) in benzene (20 mL) was heated with refluxing. Catalytic amount of *p*-toluenesulfonic acid monohydrate was added to the solution, and the reaction mixture was stirred for 5 min. The mixture was cooled on an ice-bath. The crude product was purified by column chromatography on silica gel [benzene/hexane (1:4, v/v)] to give **14** (41.6 mg, 81%) as orange powder: ^{1}H NMR (270 MHz, $CDCl_3$) δ 8.54 (br s, 2H), 8.29 (s, 2H), 8.24 (s, 2H), 7.57 (dt, J = 10.3, 2.3 Hz, 2H), 6.46 (dt, J = 10.3, 4.3 Hz, 2H), 4.17 (m, 4H), 1.66, 1.65 (s, s, 36H); FD MS *m*/*z* 626 (M^+).

4,8,12,16-Tetra-*tert*-butyl-*s*-indaceno[1,2,3-*cd*:5,6,7-*c*′*d*′]diphenalene (5). A mixture of **14** (41.6 mg, 66.4 mmol) and *p*-chloranil (18.1 mg, 73.6 mmol) in benzene (70 mL) was refluxed for 40 min. The mixture was cooled on an ice-bath and concentrated in vacuo. The crude product was purified by column chromatography on silica gel [benzene/hexane (1:4, v/v)] followed by recrystallization to give **5** (32.2 mg, 78%) as green prisms: mp > 300 °C; ^{1}H NMR [400 MHz, CS_2/acetone-d_6 (4:1, v/v)] δ 7.69 (d, J = 8.4 Hz, 2H), 7.10 (s, 2H), 7.04 (s, 4H), 6.98 (t, J = 8.4 Hz, 4H), 1.51 (s, 36H); FD MS *m*/*z* 624 (M^+). Anal. Calcd for $C_{48}H_{48}$: C, 92.26; H, 7.74. Found: C, 92.29; H, 7.79.

Dication (5^{2+}). The hydrocarbon **5** (5 mg, 8 mmol) was added to 0.5 mL of concentrated D_2SO_4 to give a dication species. A reddish purple color appeared immediately. The dication was also obtained as reddish purple plates by the reaction of **5** (22.5 mg, 36 mmol) with excess $SbCl_5$ (0.05 M, 2.88 mL, 144 mmol) in 22.5 mL of CH_2Cl_2.

Radical cation ($5^{(\bullet)(+)}$). The radical cation was generated by the reaction of **5** (22.5 mg, 36 mmol) with an equimolar amount of $SbCl_5$ (0.05 M, 0.72 mL, 36 mmol) in 22.5 mL of CH_2Cl_2. The solution turned greenish blue immediately.

Radical anion ($5^{(\bullet)(-)}$). The radical anion was generated under vacuum (ca. 10^{-4} Torr) in sealed cell by the reaction of **5** with a potassium mirror in DME or THF.

Dianion (5^{2-}). The reaction of dihydro compounds **14** (7.5 mg, 12 mmol) with a potassium mirror in THF-d_8 (0.5 mL) in a sealed degassed tube afforded dianion species. The dianion was also obtained by the reaction of **5** with a potassium mirror in THF in a sealed degassed tube.

5·TCNQ Complex. The solution of **5** (11.4 mg, 18.3 mmol) and TCNQ (7.3 mg, 36.5 mmol) in CH_2Cl_2 (11 mL) was allowed to stand at 5 °C for 4 days. The resulting green needles (10.5 mg, 70%) were collected: mp > 300 °C; IR (KBr) 2214 cm^{-1}. Anal. Calcd for $C_{60}H_{52}N_4$: C, 86.92; H, 6.32; N, 6.76. Found: C, 86.31; H, 6.14; N, 6.83. The material for elemental analysis was dried under vacuum at 100 °C for 1 day.

ESR Spectroscopy. Neutral (5). The compound **5** was purified by column chromatography (silica gel) and then recrystallized from benzene to give green prisms. For the solution state studies, a solution of **5** (2×10^{-4} M, 0.2 mL) in toluene was introduced into the cell by a syringe. The cell was connected to a vacuum line and the solvent was degassed by a repeated freeze−pump−thaw method (five times). The cell was sealed, and the ESR spectra of **5** were recorded. For the solid-state studies, the solid **5** (5 mg) was introduced into the cell, and the cell was connected to a vacuum line. The cell was sealed, and the ESR spectra of the solid **5** were recorded.

Radical Cations ($5^{(\bullet)(+)}$). A solution of $5^{(\bullet)(+)}$ (2×10^{-4} M, 0.2 mL) in CH_2Cl_2 was introduced into the cell by a syringe. The cell was connected to a vacuum line, and the solvent was degassed by a repeated freeze−pump−thaw method (five times). The cell was sealed, and the ESR spectra of radical cations were recorded.

Radical Anions ($5^{(\bullet)(-)}$). A clean piece of potassium was passed into the sidearm and sealed. A solution of **5** (5×10^{-4} M, 0.2 mL) in DME was introduced into the cell by a syringe. The cell was connected to a vacuum line and then the solvent was degassed by a repeated freeze−pump−thaw method (five times). The sidearm was warmed with a luminous flame to distill the metal as a mirror onto the walls. The sidearm was removed by sealing. Finally, the cell was sealed. The contact of the solution with a potassium mirror at room temperature gave the radical anion.

UV−Vis−Near-IR spectroscopy. Dication (5^{2+}). The quantitative electronic spectrum of 5^{2+} was obtained by the dissolution of the solid **5** (1.0859 mg, 1.7377 mmol) in D_2SO_4 (100 mL) at room temperature.

Radical Cation ($5^{(\bullet)(+)}$). The qualitative measurement was carried out in the CH_2Cl_2 solution of $5^{(\bullet)(+)}$ at room temperature.

Neutral (5). The compound **5** was purified by a column chromatography (silica gel) and then recrystallized from benzene to give green prisms. The pure **5** was dissolved in a mixture of CH_2Cl_2 and cyclohexane (100 mL, 1:100), and the quantitative measurement was carried out at room temperature.

Dianion (5^{2-}) and Radical Anion ($5^{(\bullet)(-)}$). A clean piece of potassium was passed into the sidearm, and the sidearm was sealed. The solution of **5** in THF was introduced into the cell by a syringe.

The cell was connected to a vacuum line, and then the solvent was degassed by a repeated freeze−pump−thaw method (five times). The sidearm was warmed with a luminous flame to distill the metal as a mirror onto the walls. The sidearm was removed by sealing. Finally, the cell was sealed. The contact of the solution with a potassium mirror at room temperature exhibited the gradual decrease of absorption of **5**, and the new absorptions attributable to $\mathbf{5}^{(\bullet)(-)}$ appeared. Further contact with a potassium mirror caused the gradual decrease of the absorption of $\mathbf{5}^{(\bullet)(-)}$ with the gradual increase of the absorption of $\mathbf{5}^{2-}$.

Acknowledgment. This work was supported by a Grant-in-Aid for Scientific Research on Priority Areas (No. 06218217) from the Ministry of Education, Science and Culture, Japan.

Supporting Information Available: Preparative procedures and spectroscopic data for 4,7-di-*tert*-butyl-5/6-methylacenaphthen-1-ol and 4,7-di-*tert*-butyl-5-methylacenaphthenequinone, the NMR spectra of **5**, the ESR spectra of $\mathbf{5}^{(\bullet)(+)}$ and $\mathbf{5}^{(\bullet)(-)}$, X-ray data (molecular strucures, bond lengths, bond angles) for **5** and **5**·TCNQ complex, and the electronic absorption spectra of the **5**-TCNQ complex (7 pages). See any current masthead page for ordering information and Web access instructions.

JA970961M